J. Phys.: Condens. Matter 4 (1992) 10105–10116. Printed in the UK

Structure and Brownian dynamics of the two-dimensional Yukawa fluid

Hartmut Löwen

Sektion Physik der Universität München, Theresienstraße 37, D-8000 München 2, Federal Republic of Germany

Received 29 June 1992, in final form 21 September 1992

Abstract. The two-dimensional Yukawa pair potential represents a simple model for the interaction of charge-stabilized colloidal particles confined between two charged plates. Static and dynamical correlations in the liquid state of this model are calculated using Brownian dynamics simulations. In particular, the pair, triplet and orientational structure are discussed as well as dynamical quantities like particle diffusion and the time-dependence of the nearest-neighbour orientational correlation. It is found that the decay of nearest-neighbour orientation is non-exponential in time. Its relaxation occurs on a time scale that is much larger than a time typical for the crossover of the translational diffusion to the hydrodynamic regime.

1. Introduction

The investigation of the structure and dynamics of colloidal suspensions has become a field of intense research and increasing interest during the last decades. Both scattering experiments and theories involving models from statistical mechanics were used to explore static and dynamical phenomena, (see references [1–3] for recent reviews). It turned out that the experimental data could often be understood in terms of relatively simple models with a pairwise potential: a hard-sphere potential for sterically stabilized and the so-called Derjaguin–Landau–Verwey–Overbeek (DLVO) [4] potential for charge-stabilized colloidal suspensions. The electrostatic part of the latter is simply of Yukawa form with the Debye–Hückel screening length. Thus there are now well-characterized experimental systems on a mesoscopic length scale for simple theoretical models with a pairwise potential.

Recently, it has also become possible to prepare *two-dimensional* colloidal systems, i.e. colloidal particles moving in thin water films on a substrate or between two parallel glass plates. By optical microscopy and digital image processing [5–10] one can directly visualize typical configurations and particle trajectories and thus gain direct insight into the real-space structure and dynamics of the two-dimensional system. As regards charge-stabilized colloidal particles (macroions), they are usually confined between highly charged plates and are thus well restricted to the two dimensions parallel to the plates. On the other hand, sterically stabilized colloidal particles can also move perpendicular to the confining plates and this additional dimension can be controlled by the distance between the plates. As in the three-dimensional case a hard-sphere or a DLVO-type potential, respectively, is an appropriate description of the particle

0953-8984/92/5010105+12$07.50

interactions. In the case of highly charged plates, the van der Waals interaction is negligible compared to the strong electrostatic repulsion and a simple Yukawa potential describes the dominant interaction (see Chang and Hone [11]).

The dynamics of a colloidal suspension is Brownian rather than Newtonian due to solvent friction. If the suspension is dilute enough, hydrodynamic interactions can safely be ignored and simple Brownian motion of interacting particles is an appropriate picture for the dynamics. Whereas both the Yukawa [12, 13] and the hard-sphere model [14] with simple Brownian motion have been studied extensively by Brownian dynamics (BD) simulations in three dimensions, little attention has been paid until now to their two-dimensional or quasi-two-dimensional reductions. Recently, Schaertl and Sillescu [10] studied particle self-diffusion in the quasi-two-dimensional hard-sphere model by a BD simulation and found agreement with their own experimental data. But the two-dimensional Yukawa fluid has not yet been studied systematically.

In this paper, an extensive BD simulation for the two-dimensional Yukawa fluid is presented. There are several reasons that have motivated this study. First, the 'exact' simulation data provide a severe test for theories regarding the structure and dynamics of Yukawa liquids [15, 16]. Second, one could try to fit the experimental data (e.g. the two-dimensional pair correlation function $g(r)$) with an effective charge of a Yukawa potential, to predict then different structural and dynamical quantities by the simulations and to compare again with the experiment. Third, a two-dimensional liquid which undergoes Brownian dynamics is interesting in itself. The peculiarity of a two-dimensional system is that the nearest-neighbour orientational correlation is simply defined and plays a key role in characterizing two-dimensional melting (for a review, see [17]). One interesting question concerns the time-scale on which this orientation decays in comparison with the time where the translational diffusion reaches the hydrodynamic regime, i.e. the regime where particle motion can be characterized by the long-time self-diffusion coefficient D_∞. It is found that the relaxation of orientation in a strongly interacting liquid is considerably slower than the relaxation to long-time diffusion.

The paper is organized as follows: in section 2, the model and the Brownian dynamics simulation method are introduced and briefly explained. Then, results for the pair, triplet and orientational structure are given in section 3. In particular, the results for the triplet correlations are compared with Kirkwood's superposition principle for the three-particle distribution function. Furthermore, dynamical correlations are discussed in section 4. The paper concludes with a summary and an outlook.

2. The model and simulational method

We consider a charged colloidal suspension between two highly charged parallel plates and we assume an effective two-dimensional Yukawa potential between the macroions. Usually it is written as

$$V(r) = (Z^{*2}e^2/\epsilon r)\exp(-\kappa r) \tag{1}$$

where Z^*e is an effective charge, ϵ is the dielectric constant of the solvent and κ is the inverse screening length. Chang and Hone [11] have shown that the screening

length is dominated by the counterions of the charged plates if their surface charge is high, i.e. for a charge density σ of about $\sigma \gtrsim 10^{14} e\,\mathrm{cm}^{-2}$. Under these circumstances κ is simply given by

$$\kappa = \pi/\sqrt{2}d \tag{2}$$

where d is the distance between the plates. For a two-dimensional colloidal suspension, the relation of the effective charge Z^*e to microscopic quantities is not known exactly at the moment. This is in contrast to the usual three-dimensional case where the DLVO-model or the Poisson–Boltzmann-cell model (see [18,2]) give explicit expressions for Z^*. However, as is often done in the three-dimensional case, one can treat Z^* as a free parameter to fit certain experimental data. Typical values of Z^* are between 100 and 10000.

In writing down the two-dimensional Yukawa model (1), we have made several approximations. First, the plates must be highly charged in order to justify the confinement of particle motion to two dimensions and also to guarantee the expression (2) for κ. Next, we have neglected image-charge effects on the plates which would make the interaction more repulsive, but for large $d/\rho^{-1/2}$, where $\rho = N/A$ is the area density of the colloidal particles, the corrections are negligible, see [19]. Of course one could also study the full effective potential where all image charges are taken into account, as given explicitly by Chang and Hone [19], but this would spoil the simplicity of our simple Yukawa model somewhat. Another inherent assumption is the pair potential picture. Recent work for three-dimensional colloids [20] indicates that effective counterion-induced many-body forces become relevant for concentrated charged colloids. However, for relatively small densities, a pair potential picture (at least with one adjustable parameter Z^*) should be sufficient.

Let us now describe briefly the Brownian-dynamics simulation method which is fairly standard [21, 13]. The irreversible coupled equations of motion for the N colloidal particle positions $\{\boldsymbol{r}_i(t), i = 1, \ldots, N\}$ read

$$\xi \dot{\boldsymbol{r}}_i(t) = \boldsymbol{F}_i(t) + \boldsymbol{R}(t) \tag{3}$$

where

$$\boldsymbol{F}_i = -\nabla_i \sum_{j \neq i} V(|\,\boldsymbol{r}_i - \boldsymbol{r}_j\,|) \tag{4}$$

is the effective total interparticle force and $\boldsymbol{R}(t)$ is the Langevin random force of the solvent. ξ is the friction coefficient and sets the time scale τ_B for the macroions. It is also related to the short-time diffusion coefficient D_0 via $D_0 = k_B T/\xi$ where T is the temperature (usually room temperature). In the following, we have chosen the time scale τ_B arbitrarily to be

$$\tau_B = \xi\epsilon \exp(\kappa/\sqrt{\rho})/(\rho^{3/2} Z^{*2} a_B E_H) \tag{5}$$

where $a_B = 0.53\,\text{Å}$ is the Bohr radius and $E_H = 27\,\mathrm{eV}$ is the Hartree energy.

Finite difference integration of equation (3) leads to

$$\boldsymbol{r}_i(t + \Delta t) = \boldsymbol{r}_i(t) + (1/\xi)\boldsymbol{F}_i(t)\Delta t + (\Delta \boldsymbol{r})_R + O((\Delta t)^2) \tag{6}$$

Table 1. Parameters of different runs. The dielectric constant $\epsilon = 78$, the temperature $T = 300\,\mathrm{K}$, the effective macroion charge $Z^* = 470$ and the screening parameter $\kappa = 2.34 \times 10^6\,\mathrm{m}$ are fixed. Given are the density ρ in $\mu\mathrm{m}^{-2}$, the equation of state $Z = P/\rho k_B T$, the reduced long-time diffusion constant $D^* = D_\infty/D_0$ and the value g_{max} of $g(r)$ at the first maximum. All runs are in the liquid state except run G which corresponds to a triangular crystal.

Run	ρ	Z	D^*	g_{max}
A	0.255	7.6	0.33	1.70
B	0.51	26.1	0.171	2.45
C	0.56	30.9	0.16	2.57
D	0.61	35.9	0.14	2.67
E	0.77	52.4	0.072	3.0
F	0.92	70.5	0.05	3.4
G	1.38	—	0.00	4.3

where the random displacement $(\Delta r)_R$ is sampled from a Gaussian distribution of zero mean and variance $\overline{(\Delta r)_R^2} = 4D_0\Delta t$. The typical order of Δt was $0.0015\tau_B$. We have done a series of runs for different densities $\rho = N/A$, but fixed potential parameters. The data of the different runs are explicitly given in table 1. $N = 440$ or $N = 1764$ particles were equilibrated in a square with periodic boundary conditions and then statistics were gathered for typically 50 000 timesteps. All results were the same for $N = 440$ and $N = 1764$.

As a final remark, hydrodynamic interactions are ignored by assuming the simple Brownian-dynamics algorithm (6). In order to get an estimation of the relevance of hydrodynamic interactions, one can consider the ratio of the short-time diffusion coefficient D_0 to the first off-diagonal correction term of the e.g. Rotne–Prager diffusion matrix [1] for a particle of radius R at mean separation $\sqrt{\rho}$. This ratio is of the order of $R/\sqrt{\rho}$; in a dilute though strongly interacting suspension of highly charged particles it is less than one percent. Furthermore, hydrodynamic interactions between the plates and the particles are of the order of R/d and are therefore only negligible if the particles are far enough from the plates. Normally, d is of the same order of magnitude as the interparticle spacing; thus hydrodynamic interactions can be ignored for a dilute suspension.

3. Results for the structures

In table 1, the parameters for the different runs are listed. We take fixed parameters for the Yukawa potential (in fact, the same parameters as in [11], typical for a two-dimensional colloidal suspension) and we vary the area density ρ. The temperature $T = 300\,\mathrm{K}$ is fixed, too. Seven different runs corresponding to different area density ρ were done.

3.1. Pair structure

The two-dimensional pair correlation function $g(r)$ is defined as usual by

$$g(r) = \frac{1}{\rho}\left\langle \frac{1}{N} \sum_{i,j=1;i\neq j}^{N} \delta(r - r_i + r_j) \right\rangle \tag{7}$$

where $\langle \ldots \rangle$ is a canonical average. Results for this quantity are given in figure 1 for runs A, B, E and G. With increasing density, the structure becomes more pronounced, but the finite-size state remains liquid-like up to $\rho \simeq 1.0\ \mu m^{-2}$ and then freezes into a triangular crystal. For comparison, a typical spherically averaged pair-correlation function in the crystalline state is also shown in figure 1, exhibiting a split second peak due to the nearest-neighbour shells of the triangular lattice.

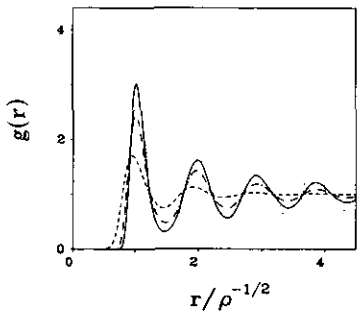

Figure 1. Pair-correlation function $g(r)$ versus reduced distance $r/\rho^{-1/2}$ for run A (dashed line), run B (dot-dashed line) and run E (solid line). For comparison, the spherically averaged $g(r)$ for the triangular crystal of run G is also given (dotted line).

We have also checked the number of nearest and next-nearest neighbours, N_n and N_{nn}, respectively. They are obtained by integrating $g(r)$ as

$$N_n = 2\pi\rho \int_0^{R_1} \mathrm{d}r\, r g(r) \tag{8}$$

and

$$N_{nn} = 2\pi\rho \int_{R_1}^{R_2} \mathrm{d}r\, r g(r) \tag{9}$$

where R_1, R_2 are the positions of the first and second minimum of $g(r)$. N_n is always very close to 6, whereas N_{nn} is close to 12 in the liquid phase. This indicates that the short-range order in the liquid resembles that of a triangular crystal.

From the virial expression, one can also compute the pressure P, or the equation of state Z, of the two-dimensional system as

$$Z \equiv \frac{P}{k_B T \rho} = 1 - \frac{\rho\pi}{2k_B T} \int_0^{\infty} \mathrm{d}r\, r^2 g(r) \frac{\mathrm{d}V}{\mathrm{d}r}. \tag{10}$$

Results for Z are given in table 1. Obviously, Z increases with density. A detailed knowledge of Z allows the calculation of thermodynamic quantities and is also needed as an input for density-functional calculations of inhomogeneous situations.

One point that makes a two-dimensional colloidal liquid very attractive from an experimental point of view is that $g(r)$ is directly accessible by evaluating typical configurations in real space obtained by digital image processing. This is very much different from the case of three-dimensional atomic or colloidal liquids where scattering techniques yield only direct information on the structure in Fourier space and a measurement of $g(r)$ suffers from cut-off errors in a Fourier transformation to real space. Thus real-space correlations can in principle be directly compared to the experimental results.

3.2. Triplet structure

Whereas the pair-correlation function measures two-particle correlations, we are now considering three-body correlations. These are much more sensitive to details of the interparticle forces than the pair structure and therefore a comparison of experimental data with our simulational results can reasonably test the validity of the Yukawa model. A convenient quantity to characterize triplet correlations is the distribution function of the bond angle θ of particle triplets which have one interparticle distance smaller than r_1 and another interparticle distance smaller than r_2. θ is then the angle between these two interparticle distances. The distribution function of θ is called $g_3(\theta, r_1, r_2)$ and it is conveniently normalized such that its θ-integral equals unity. $g_3(\theta, 0, R_1)$ measures bond angle distributions in the nearest-neighbour shell, whereas $g_3(\theta, R_1, R_2)$ gives this distribution of the origin particle with its next-nearest-neighbour shell. Here, R_1, R_2 denote the position of the first and second minimum of $g(r)$.

$g_3(\theta, 0, R_1)$ is shown in figure 2(*a*). It exhibits pronounced maxima at $\theta \approx 60°, 120°, 180°$, indicating a latent triangular structure already in the liquid that increases with increasing density. $g_3(\theta, R_1, R_2)$, on the other hand, has peaks at multiples of 30° and is shown in figure 2(*b*).

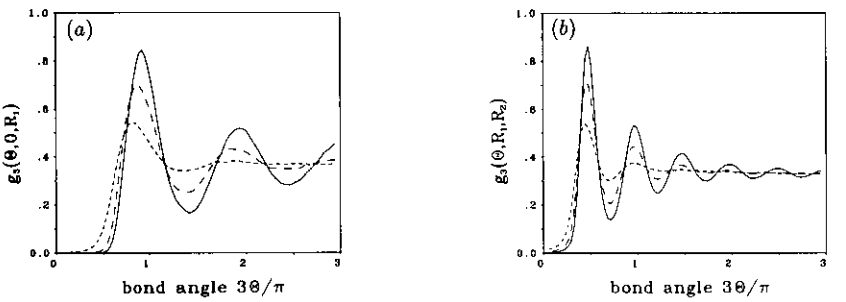

Figure 2. (*a*) Bond-angle distribution function $g_3(\theta, 0, R_1)$, R_1 being the position of the first minimum of $g(r)$, versus bond angle θ. θ is given in units of $\pi/3 = 60°$. The units of $g_3(\theta, 0, R_1)$ are such that its θ-integral is normalized: $\int_0^\pi d\theta\, g_3(\theta, 0, R_1) = 1$. Results are given for runs A, B and E; the line types are as in figure 1. (*b*) Same as (*a*) but now for $g_3(\theta, R_1, R_2)$ where R_2 is the position of the second minimum of $g(r)$.

A familiar approximation of triplet correlations is Kirkwood's superposition [22]. It consists in approximating the three-particle distribution function $g_3(\boldsymbol{r}_1, \boldsymbol{r}_2, \boldsymbol{r}_3)$ [23] by the factorization

$$g_3(\boldsymbol{r}_1, \boldsymbol{r}_2, \boldsymbol{r}_3) = g(|\boldsymbol{r}_1 - \boldsymbol{r}_2|)g(|\boldsymbol{r}_1 - \boldsymbol{r}_3|)g(|\boldsymbol{r}_2 - \boldsymbol{r}_3|). \tag{11}$$

Originally, this was proposed for three-dimensional liquids. A comparison of Kirkwood's principle with simulational data has not been done until now for 2D liquids, although it is interesting both from a theoretical and calculational point of view. In this approximation, one obtains

$$g_3(\theta, r_1, r_2) = \frac{\int_{r_1}^{r_2} dr \int_{r_1}^{r_2} dr' rr' g(r)g(r')g(\sqrt{r^2 + r'^2 - 2rr'\cos\theta})}{\int_0^\pi d\theta \int_{r_1}^{r_2} dr \int_{r_1}^{r_2} dr' rr' g(r)g(r')g(\sqrt{r^2 + r'^2 - 2rr'\cos\theta})}. \tag{12}$$

In figure 3, the results for run E are compared with Kirkwood's superposition. The structure of the low-angle peaks ($\theta \lesssim \pi/2$) is reproduced satisfactorily, whereas Kirkwood's superposition fails to predict the structure for high angles $\theta \gtrsim \pi/2$. In other words, Kirkwood's superposition principle only works for small-distance triplet correlations.

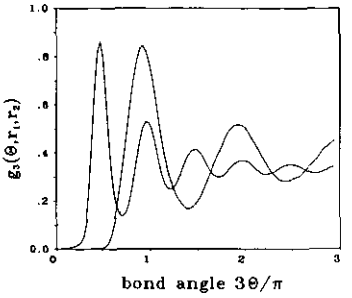

Figure 3. The results of run E (solid lines) for both $g_3(\theta, 0, R_1)$ (i.e. $r_1 = 0$, $r_2 = R_1$) and $g_3(\theta, R_1, R_2)$ (i.e. $r_1 = R_1$, $r_2 = R_2$) are compared with Kirkwood's superposition approximation for triplet correlations (dotted lines).

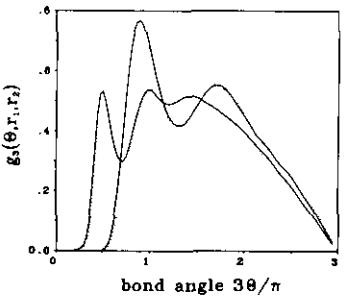

Figure 4. Same as figure 3, but now for a three-dimensional Yukawa liquid. The potential and the temperature are as in figure 3, whereas the three-dimensional density is $\rho^{3/2}$, where ρ is the two-dimensional density from figure 3.

Let us also discuss the accuracy of Kirkwood's superposition principle in *three* dimensions [24]. The bond-angle distribution can readily be defined in three dimensions and Kirkwood's approximations reads

$$g_3(\theta, r_1, r_2) = \frac{\sin\theta \int_{r_1}^{r_2} \mathrm{d}r \int_{r_1}^{r_2} \mathrm{d}r'\, r^2 r'^2 g(r) g(r') g(\sqrt{r^2 + r'^2 - 2rr'\cos\theta})}{\int_0^{\pi} \mathrm{d}\theta \sin\theta \int_{r_1}^{r_2} \mathrm{d}r \int_{r_1}^{r_2} \mathrm{d}r'\, r^2 r'^2 g(r) g(r') g(\sqrt{r^2 + r'^2 - 2rr'\cos\theta})} \tag{13}$$

where $g(r)$ is now the three-dimensional pair-correlation function. In figure 4, we compare the data of a three-dimensional Yukawa simulation (solid line) with Kirkwood's superposition (dotted line). In order to get a comparable structure, the same potential and the same temperature as in figure 3 were used and the three-dimensional density was chosen to be $\rho^{3/2}$ where ρ is the area density of figure 3. As can be clearly seen in figure 4, Kirkwood's approximation describes three-dimensional triplet correlations within the first shell of nearest neighbours reasonably even for higher bond angles. This results from the additional azimuthal average over particle triplets. As in 2D, Kirkwood's approximation gives deviations for larger bond angles in the next-nearest-neighbour shell. However, the failure in two dimensions is more dramatic since there is a considerable mismatch in the oscillations of the bond-angle distribution. Therefore, for high bond angles, Kirkwood's superposition principle works better in three than in two spatial dimensions.

In contrast to the three-dimensional case, where only indirect experimental information on triplet correlations is known, the bond-angle distribution function $g_3(\theta, r_1, r_2)$ is directly accessible in experiments on two-dimensional liquids, as the particle-configurations are available. Until now, experimental attention was mainly focused on functions like $g(r)$ and $g_6(r)$ which are discussed later. It would, however, also be an interesting experimental task to verify the strong oscillations in the bond-angle distribution and to compare them with the present simulational data.

3.3. Nearest-neighbour orientational correlations

Nearest-neighbour orientational correlations in a two-dimensional fluid are conveniently measured by the orientational correlation function $g_6(r)$ which is an order parameter for a sixfold symmetry:

$$g_6(r) = \frac{1}{\rho}\left\langle \frac{1}{N} \sum_{i,j=1;i\neq j}^{N} \delta(r - r_i + r_j)\Psi_i \Psi_j^* \right\rangle. \tag{14}$$

Here,

$$\Psi_j = \frac{1}{6}\sum_{m=1}^{6} \exp(i6\theta_{jm}) \tag{15}$$

where the sum goes over the six nearest neighbours of particle j and θ_{jm} is the angle between the bond joining the jth and the mth particle and some fixed axis. In the liquid phase, $g_6(r)$ decays exponentially whereas in a possible *hexatic* phase $g_6(r)$ has an algebraic decay. A plot of $g_6(r)$ for run E is given in figure 5. As the pair-correlation function $g(r)$, it oscillates and then decays to zero. It even has small negative values for positions corresponding to the first minimum of $g(r)$. A plot of $\ln(g_6(r))$ versus r falls reasonably well on a straight line for large r so that run E represents a liquid. Therefore the runs A, B, C and D which have lower densities than run E are also liquid and not hexatic.

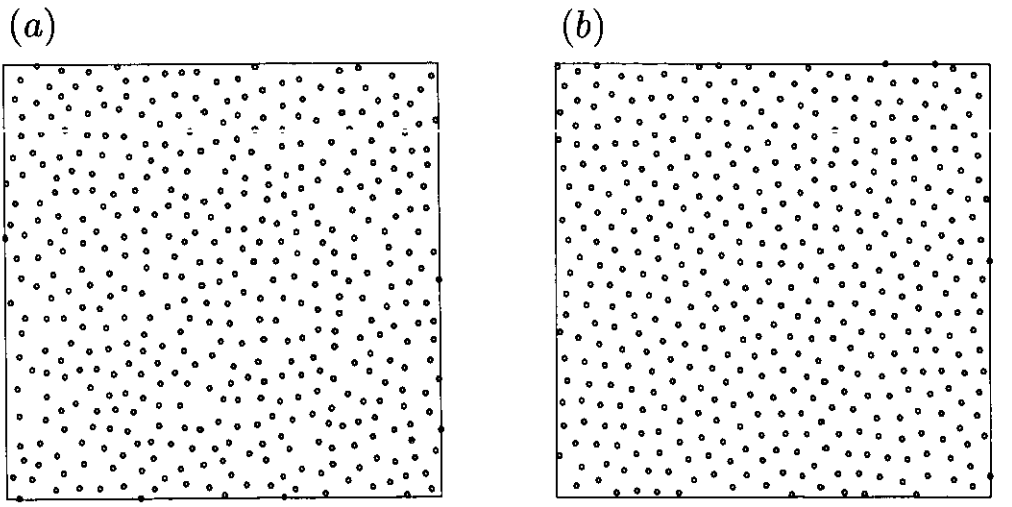

Figure 5. Orientational correlation function $g_6(r)$ as defined in the text versus reduced distance $r/\rho^{-1/2}$ for run E.

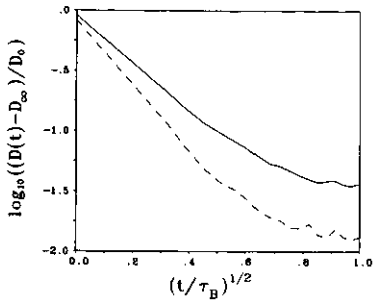

Figure 6. Typical configurations of 440 particles in a square with periodic boundary conditions; (*a*) for run A, (*b*) for the dense liquid of run E. Here an increase of neighbouring orientation can clearly be seen.

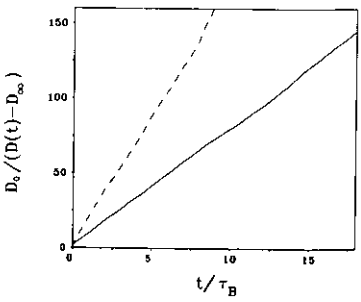

Figure 7. Inverse of the reduced time-dependent diffusion constants $D_0/(D(t) - D_\infty)$ versus reduced time t/τ_B for runs B (dot-dashed line) and E (solid line).

3.4. Typical configurations

In figure 6, we show typical configurations of the two-dimensional Yukawa fluid for runs A and E. What can be seen directly is the fact that the orientational as well as the positional order increases as the density increases. Whereas there are voids in run A, the configuration of run E exhibits a marked orientational correlation over several interparticle spacings. Again, similar two-dimensional configurations can be obtained experimentally, see e.g. [8,9].

4. Brownian dynamics and time-dependent correlations

The first interesting quantity, characterizing particle self-diffusion, is the time-dependent diffusion constant $D(t)$, defined as

$$D(t) = (1/4t)\,W(t) \tag{16}$$

where

$$W(t) = \left\langle \frac{1}{N}\sum_{i=1}^{N}(\boldsymbol{r}_i(t) - \boldsymbol{r}_i(0))^2 \right\rangle \tag{17}$$

is the mean-square particle displacement. Alternatively, one can also define a time-dependent diffusion constant by the differential expression

$$\overline{D}(t) = (1/4)(\mathrm{d}/\mathrm{d}t)W(t). \tag{18}$$

Clearly, for $t = 0$, the short-time diffusion coefficient induced by the solvent is obtained

$$D(t = 0) = \overline{D}(t = 0) = D_0. \tag{19}$$

For long times, the two expressions also yield the same value, namely the long-time self-diffusion coefficient D_∞:

$$\lim_{t\to\infty} D(t) = \lim_{t\to\infty} \overline{D}(t) = D_\infty. \tag{20}$$

Data for D_∞ are given in table 1. Remarkably, D_∞ is finite for Brownian dynamics in two dimensions whereas it is infinite for two-dimensional molecular dynamics [25]. Furthermore, a theoretical analysis [26] shows that

$$D(t) - D_\infty = O(1/t) \qquad \overline{D}(t) - D_\infty = O(1/t) \tag{21}$$

so there is a $1/t$ long-time tail in both $D(t)$ and $\overline{D}(t)$. We have tried to fit the simulational data for $D(t)$ and $\overline{D}(t)$ using different analytical expressions in order to extract a typical relaxation time needed to cross over to the hydrodynamic regime where $D(t), \overline{D}(t) \simeq D_\infty$. A good fit was obtained by using the algebraic expression

$$D(t) = D_\infty + A/(t + t_R). \tag{22}$$

In figure 7, it is shown that a plot of $D_0/(D(t) - D_\infty)$ versus t does indeed fall reasonably well on a straight line. The expression (22) also reproduces the correct long-time tail (21). Values for the fit parameters A and t_R are summarized in table 2. We add as a remark that fit-functions for $\overline{D}(t)$ always yield typical relaxation times that are a bit smaller than t_R so that t_R is an upper bound on a typical relaxation time for the crossover of particle self-diffusion to the hydrodynamic regime.

Table 2. Parameters of the algebraic fit $A/(t + \tau_0)$ for the translational diffusion $(D(t) - D_\infty)/D_0$ and parameters of the stretched exponential fit $A\exp(-\sqrt{t/\tau_0})$ for the nearest-neighbour orientational autocorrelation function $p(t)/p(0)$.

Run	Fitted function	A	τ_0
B	$(D(t) - D_\infty)/D_0$	0.06	0.22
B	$p(t)/p(0)$	0.07	1.1
E	$(D(t) - D_\infty)/D_0$	0.13	0.29
E	$p(t)/p(0)$	0.1	4.0

An interesting question concerns the time-dependence of the nearest-neighbour orientational correlation. We define the autocorrelation function of particle orientation as

$$p(t) = \left\langle \frac{1}{N} \sum_{j=1}^{N} \Psi_j(0)\Psi_j^*(t) \right\rangle \tag{23}$$

where

$$\Psi_j(t) = \frac{1}{6} \sum_{m=1}^{6} \exp(i6\theta_{jm}(t)) \tag{24}$$

and the notation is as in (15). $p(t)$ measures the decay of a given orientation of a particle with respect to its six nearest neighbours. The logarithm of the normalized quantity $p(t)/p(0)$ is plotted in figure 8 versus $\sqrt{t/\tau_B}$ for runs B and E. The resulting curves fall very well on a straight line showing that a stretched exponential fit with exponent $\frac{1}{2}$ is adequate at least for intermediate times t

$$p(t)/p(0) \simeq A\exp(-\sqrt{t/\tau_p}). \tag{25}$$

Definitively, the decay of $p(t)$ is not a *simple* exponential in time as reflected by the low stretching exponent $\frac{1}{2}$. However, we emphasize that (25) is only one possible intermediate-time fit which may fail for very large times where algebraic tails could become relevant. Unfortunately no exact statements about such long-time tails are known at present for $p(t)$. Results for the fit parameters A and τ_p are given in table 2. From these data, it becomes clear that the inherent time τ_p for the relaxation of the orientational correlation is much larger than the relaxation time τ_R of the translational diffusion describing the crossover to the hydrodynamic regime. This fact is expected for a hexatic phase, but less evident for a liquid phase. It shows that even in the liquid the orientation is a much more persistent quantity than translational correlations. Finally, the ratio τ_p/τ_R is increasing for increasing density.

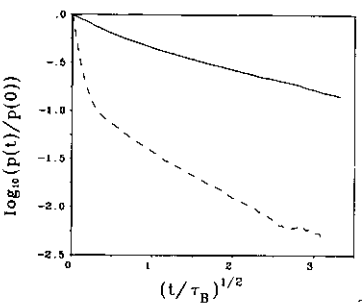

Figure 8. Logarithm of the nearest-neighbour orientational correlation $p(t)/p(0)$ as defined in the text versus square root of the reduced time t/τ_B for runs B and E. The line types are as in figure 7.

5. Summary and outlook

In this paper, the two-dimensional Yukawa liquid was simulated using Brownian-dynamics simulations. Results for the structure and dynamics were obtained that could be compared with experiments on charged colloids confined between highly charged parallel plates and that provide also a test for possible theories of liquid structure and dynamics in two spatial dimensions. I hope that the paper has an impact in two directions. First, in experiments, a more detailed analysis with the configuration data could give detailed results for the bond-angle distribution which can then, in turn, be compared with the simulations, and an analysis of different time-dependent configurations should confirm the slower relaxation of nearest-neighbour orientations than that of self-diffusion in strongly interacting liquids. Second, the data for the long-time self-diffusion can be compared with recent theoretical expressions from kinetic theory for continuous potentials. One work has already been started in this direction and will be published elsewhere [27].

A remaining question concerns the location of the crystallization line towards a triangular crystal for a large but finite system. Another open direction is a systematic examination of a possible hexatic phase in the 2D Yukawa system. Also, as a more fundamental problem, the Yukawa pair-potential assumption (1) may be questioned. It is tempting to use a combination of density-functional theory and molecular dynamics that includes effective many-body forces between the macroions which are induced by the counterions and the charged plates. Our future work lies in this direction.

Acknowledgments

I thank R Klein and G Szamel for helpful discussions.

References

[1] Pusey P N 1991 *Liquids, Freezing and the Glass Transition* ed J P Hansen *et al* (Amsterdam: North Holland)
[2] Sood A K 1991 *Solid State Phys.* **45** 1
[3] ed Chen S-H, Huang J S and Tartaglia P 1992 *Structure and Dynamics of Strongly Interacting Colloids and Supramolecular Aggregates in Solution (Nato ASI Series)* (Dordrecht: Reidel)
[4] Verwey E J W and Overbeek J Th 1948 *Theory of the Stability of Lyophobic Colloids* (Amsterdam: Elsevier)
[5] Murray C A and van Winkle D H 1987 *Phys. Rev. Lett.* **58** 1200
[6] Tang Y, Armstrong A J, Mockler R C and O'Sullivan W J 1989 *Phys Rev. Lett.* **62** 2401
[7] Armstrong A J, Mockler R C and O'Sullivan W J 1989 *J. Phys.: Condens. Matter* **1** 1707
[8] Murray C A, Sprenger W O and Wenk R A 1990 *Phys. Rev.* B **42**, 688
[9] Grier D G and Murray C A 1992 *Structure and Dynamics of Strongly Interacting Colloids and Supramolecular Aggregates in Solution (Nato ASI Series)* ed S-H Chen *et al* (Dordrecht: Reidel) pp 145–74
[10] Schaertl W and Sillescu H 1992 *J. Colloid. Interface Sci.* at press
[11] Chang E and Hone D W 1988 *Europhys. Lett.* **5** 635
[12] Gaylor K, Snook I and van Megen W 1981 *J. Chem. Phys.* **75** 1682 .
Molecular dynamics was used to study dynamical properties of the Yukawa potential by Robbins M O, Kremer K and Grest G S 1988 *J. Chem. Phys.* **88** 3286
[13] Löwen H, Hansen J P and Roux J N 1991 *Phys. Rev.* A **44** 1169
[14] Cichocki B and Hinsen K 1990 *Physica* A **166** 473; 1992 *Physica* A **187** 133
[15] Nägele G, Medina-Noyola M, Klein R and Arauz-Lara J L 1988 *Physica* A **149** 123
[16] Leegwater J and Szamel G 1992 to be published
[17] Strandburg K J 1988 *Rev. Mod. Phys.* **60** 161
[18] Alexander S, Chaikin P M, Grant P, Morales G J, Pincus P and Hone D 1984 *J. Chem. Phys.* **80** 5776
[19] Chang E and Hone D 1988 *J. Physique* **49** 25
[20] Löwen H, Madden P A and Hansen J P 1992 *Phys. Rev. Lett.* **68** 1081
[21] Ermak D L 1975 *J. Chem. Phys.* **62** 4189; 1975 **64** 4197
[22] Kirkwood J G 1935 *J. Chem. Phys.* **3** 300
[23] Hansen J P and McDonald I 1986 *Theory of Simple Liquids* 2nd edn (London: Academic)
[24] For a recent discussion of triplet correlations in three-dimensional colloidal liquids, see:
Linse P 1991 *J. Chem. Phys.* **94** 8227
[25] Alder B, Wainwright T 1970 *Phys. Rev.* A **1** 18
[26] Ackerson B J and Fleishman L 1982 *J. Chem. Phys.* **76** 2675
[27] Szamel G *et al* 1992 to be published